2E3-5

About Equivalency of Two Methods of Information Gathering in Microwave Imaging

#N. A. Simonov[1], S. I. Jeon[1], S.H. Son[1], J.M. Lee[1], H.J. Kim[1]
[1] Radio Technology Research Department, ETRI, Daejeon, South Korea
email : nsimonov@etri.re.kr

1. Introduction

Microwave imaging (MI) is an area of imaging methods when real object is illuminated by microwave signals radiating with transmitting antennas (*Tx*). Receiving antennas (*Rx*) gather information of electro-magnetic (EM) fields, scattered by this object and the reconstruction algorithms build the object image using this information. Microwave tomography (MT) system implements MI and is used for the purpose of early breast cancer detection, in particular [1]. Most of MT systems use a bath filled with a coupling liquid for better matching of antennas with the imaging object (human breast or other parts of bodies).

The quality of the reconstructed image is described by parameter of the spatial resolution, which is defined as minimal distance between any two distinguishable points of the object. Then the smaller spatial resolution, the more sharp is reconstructed image. The spatial resolution of the MT system depends on the amount of gathered information about the object. Ideally, for best quality image reconstruction, it is necessary to know a scattered EM field at some surface around the object for each its illumination. However, even in this case, the spatial resolution is usually limited by a media half-wavelength Rayleigh limit, which corresponds to the case of MT system detects propagating waves of the scattered field only. On the other hand, some papers reported about super-resolution effects in the reconstructed images [2].

For real MT systems, it is possible to measure scattered fields using *Rx* antennas placed in finite number of points. We can regards them as space sampling points that are similar to the time sampling points of time signals. Then the positions of *Tx* antennas, which produce illumination of the object, we can define as illumination points. It is clear that for higher image resolution it is necessary to gather data using multistatic multiple-input multiple-output radar concept [3] (multi illumination and multi sampling points). The same amounts of sampling/illumination points can be realized using both static arrays of *Tx*/*Rx* antennas or by scanning array with small amount of the antennas.

In this work we compared two methods of gathering information in MI using identical *Tx* and *Rx* antennas:

1) number of illumination points N_{Tx} is relatively small (7 or 15, for example), and number of sampling points N_{Rx} is relatively large (150 or 300);

2)) number of illumination points N_{Tx} is relatively large (150 or 300, for example), and number of sampling points N_{Rx} is relatively small (7 or 15).

We will compare these two methods under condition that N_{Tx} for the method 1 is equal to N_{Rx} for the method 2 and vice verse that is, keeping the same the total number of measurements $N_{Tx} \cdot N_{Rx}$.

It is clear that if the illumination points in the method 1 coincide with the sampling points in the method 2 and vice verse, the both methods are equivalent because of the reciprocity theorem. On the contrary, we regard more general case, when the illuminating and sampling points are different for both gathering methods.

More definitely, we compare application of two different circular antenna arrays having the same diameter and illuminating/sampling points are homogeneously distributed around the array circle. Our method of comparison is based on singular values decomposition (SVD) of Jacobian that in used in the Gauss-Newton image reconstruction algorithm [1, 4].

2. Method of analysis

Let us regard the measurement noises to be a random process from a standard normal distribution. Then we can write the following equation in the linear approximation, relating the vector of noises $\mathbf{n}$ in all measured signals and vector of noises $\mathbf{C}_n$ in the reconstructed contrast [1, 4]:

$$\mathbf{J}_{\mathrm{k}} \cdot \mathbf{C}_n = \mathbf{n} \tag{1}$$

Here $\mathbf{J}_{\mathrm{k}} \equiv k^2 \cdot \mathbf{J}$, where $\mathbf{J}$ is an Jacobian, calculated at Cartesian fine mesh and k is wave number in the bath liquid. We regard that noises have the same standard deviation for all measured signals and the measured data are normalized to the signals in the empty bath. Let us express SVD of the matrix $\mathbf{J}_k$ in the following standard form:

$$\mathbf{J}_k = \mathbf{U} \cdot \mathbf{S} \cdot \mathbf{V}^H \tag{2}$$

Combination and transformation of equations (1) and (2) provide to get the following relation:

$$\sigma(i) \cdot C_v(i) = n_{\mathrm{u}}(i) \tag{3}$$

Here $\sigma(i)$ is a singular value of $\mathbf{J}_k$ with index i, $\mathbf{C}_v = (\mathbf{V}^H \cdot \mathbf{C}_n)$, $\mathbf{n}_{\mathrm{u}} = (\mathbf{U}^H \cdot \mathbf{n})$.

As far as $\mathbf{n}$ is a noise for normal distribution and equations (1) - (3) are linear, the $\mathbf{C}_v$ and $\mathbf{n}_{\mathrm{u}}$ have normal distribution as well. Our investigation reveals that standard deviation $\mathbf{s}_{image}$ of vector $\mathbf{C}_v$ and standard deviation $\mathbf{s}_{meas}$ of vector $\mathbf{n}_{\mathrm{u}}$ are equal to standard deviations of vectors $\mathbf{C}_n$ and $\mathbf{n}$ correspondingly and also that $\mathbf{s}_n$ not depends on index i. Therefore, the next simple relation is following from (3):

$$\sigma(i) \cdot s_{image}(i) = s_{meas} \tag{4}$$

Let us define that the maximal acceptable noise level in the reconstructed image equal to $s_{image,max}$ and all acceptable values $s_{image}(i)$ are smaller than $s_{image,max}$. Hence from (4) we can evaluate the cutoff level for maximal acceptable singular values and effective rank r_{eff} of the matrix $\mathbf{J}_k$ [5]. Therefore, all SVD components with indexes $i \geq r_{eff}$ contribute to the reconstruction noises values, bigger than $s_{image,max}$ and are not acceptable. These statements can be expressed with the equations:

$$\sigma(i) \geq \frac{s_{meas}}{s_{image,max}} \equiv \sigma_{min} \text{ , for the acceptable } \sigma(i) \quad \Rightarrow \sigma(r_{eff}) \cong \sigma_{min} \tag{5}$$

Note that the value r_{eff} has direct relation to a mean value of the spatial resolution D [5] in the imaging zone. Namely, when the matrix $\mathbf{J}_k$ is calculated in some imaging volume ("imaging zone") the mean value D is equal to the distance between equidistant points when the total number of them in the imaging zone is equal to r_{eff}. Then

$$D = \left(V_{im\,zone}/r_{eff}\right)^{1/3} \tag{6}$$

where $V_{im\,zone}$ is a volume of the imaging zone.

If positions of *Tx/Rx* antennas are arranged in a section of the imaging zone, the matrix $\mathbf{J}_k$ can be calculated in this plane of the imaging zone only. In this case the number of such equidistant points should be calculated in this section plane only:

$$D = \left(S_{im\,zone}/r_{eff}\right)^{1/2} \tag{7}$$

where $S_{im\,zone}$ is area of the section of the imaging zone.

We calculated Jacobians $\mathbf{J}$ at 3 mm Cartesian fine mesh for the measured complex signals, normalized to signals $E_z(Tx, Rx)$ at *Rx* antennas when *Tx* transmits inside the empty bath. The formula for calculation of Jacobian $\mathbf{J}$ at fine mesh is [1, 4]:

$$\mathbf{J}(Tx/Rx, \mathbf{p}_n) = -(\Delta)^3 \cdot E_z(Tx, \mathbf{p}_n) \cdot E_z(Rx, \mathbf{p}_n)/E_z(Tx, Rx) \tag{8}$$

where $\mathbf{J}(Tx/Rx, \mathbf{p}_n)$ is an Jacobian matrix element at node $\mathbf{p}_n$ of the fine mesh when *Tx* antenna provides the illumination and *Rx* antenna provides the sampling; $E_z(Tx, \mathbf{p}_n)$ and $E_z(Rx, \mathbf{p}_n)$ are *z*-components of the electric field at the node $\mathbf{p}_n$ in the cases of the illumination with Tx and *Rx* antenna, correspondingly; Δ is the size of the fine mesh. The fields $E_z(Rx, \mathbf{p}_n)$ in (8) are excited by point sources $\mathbf{j}_z(\mathbf{r})$ with the current density [4]:

$$\mathbf{j}_z(\mathbf{r}) = -\frac{1}{i\,\omega\,\mu_0} \cdot \delta(\mathbf{r} - \mathbf{r}_{ant}) \cdot \hat{\mathbf{z}}$$

where $\delta(\mathbf{r} - \mathbf{r}_{ant})$ is the delta-function, ω is the angular frequency, μ_0 is the permeability of free-space and accent mark ^ defines unit vector. In this case the following analytical expression for the electric field in empty bath, including the near-field terms, can be applied:

$$\mathbf{E}(\mathbf{r}) = \frac{\exp(-ikR)}{4\pi R} \cdot \left[\left(1 - \mathrm{i}\frac{1}{kR} - \frac{1}{(kR)^2}\right) \cdot \bar{\bar{\mathbf{I}}} - \left(1 - \mathrm{i}\frac{3}{kR} - \frac{3}{(kR)^2}\right) \cdot \hat{\mathbf{r}}\hat{\mathbf{r}}\right] \cdot \hat{\mathbf{z}} \qquad (9a)$$

where $R = |\mathbf{r} - \mathbf{r}_{ant}|$, k is a wave-number in the bath media, $\bar{\bar{\mathbf{I}}}$ is the identity dyadic and $\hat{\mathbf{r}}\hat{\mathbf{r}}$ is a dyadic as well (eq. (7.136) in [6]). This expression becomes more simple when all nodes $\mathbf{p}_n$, *Tx* and *Rx* antennas are arranged in the same layer:

$$E_z(R) = \frac{\exp(-ikR)}{4\pi R} \cdot \left(1 - \mathrm{j}\frac{1}{kR} - \frac{1}{(kR)^2}\right) \qquad (9b)$$

3. Results of simulations

We performed simulations of the Jacobians in MATLAB using equations from the previous chapter to compare two different methods of the gathering information, described in the Introduction. For our purpose we kept the following condition:

$$N_{Tx}\,, method\ 1 = N_{Rx}\,, method\ 2$$
$$N_{Rx}\,, method\ 1 = N_{Tx}\,, method\ 2$$

Note that these equalities provide the same total number of measured signals $N_{Tx} \cdot N_{Rx}$ for both methods.

We regard circular array 150 mm in diameter and all antennas are small dipoles. The antennas are placed into the bath filled with propylene glycol 100% solution (PG100) as a coupling liquid; its dielectric properties are presented in Table 1. The testing frequencies are 900, 1500, 2100, and 2900 MHz.

Table 1. Dielectric properties of PG100 bath material

Frequency, *MHz*	permittivity	conductivity, S/m
900	11.87	0.5
1500	8.72	0.63
2100	7.42	0.73
2900	6.50	0.83

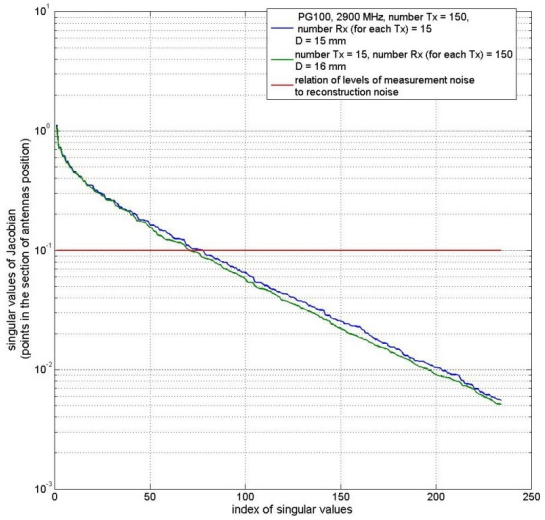

Fig. 1 Singular values of the matrix $\mathbf{J}_k$ (1), (2) for the case of array diameter 150 mm, PG100 bath liquid, N_{Tx} and N_{Rx} are equal to 150 or 15; frequency 2900 MHz. The cutoff level is 0.1.

Fig. 1 demonstrates example of plots of simulated singular values for both methods at 2900 MHz, where the cutoff line with level $\sigma_{min} = 0.1$, is showed by a horizontal line. The parameter r_{eff} is determined by an intersection of the cutoff line and the singular values graphics. Table 2 contains values D in whole simulated cases and half-wavelength Rayleigh limits D_{lim} [2, 3] of the spatial resolution:

$$D_{lim} = \frac{\pi}{|k|} \tag{10}$$

Table 2. Mean values of the spatial resolution D in mm

Frequency, *MHz*	N_{Tx} = 150, N_{Rx} = 15	N_{Tx} = 15, N_{Rx} = 150	N_{Tx} = 150, N_{Rx} = 7	N_{Tx} = 7, N_{Rx} = 150	D_{lim}
900	28	30	36	36	32
1500	23	23	28	31	24
2100	19	19	22	24	20
2900	15	16	18	18	16

Fig. 1 and Table 2 demonstrate that both methods of gathering information for MI are practically equivalent if the total amounts of measured data are the same. Table 2 demonstrates that for all testing frequencies, average values of spatial resolution are very close to their half-wavelength Rayleigh limit (10) for the bath material with losses.

4. Conclusion

We can formulate the main conclusion that both considered methods are equivalent in sense of amount of information gathering for microwave imaging. They provide the same spatial resolution of reconstructed image, if the total amounts of measured data are the same. This result, probably, can be generalized to the following rule for the microwave imaging. Namely, if we determine type of *Tx*/*Rx* antennas, the measurement noises and illumination/sampling surface and if illumination/sampling points are distributed at this surface uniformly, then the amount of gathering information depends on number of measured signals and not depends on method of information gathering.

Acknowledgment

This research was supported by the KCC (Korea Communications Commission), Korea, under the R&D program supervised by the KCA (Korea Communications Agency) (KCA-2012- 11911-01108).

References

[1] T. Rubæk, P. M. Meaney, P. Meincke, and K. D. Paulsen, " Nonlinear microwave imaging for breast-cancer screening using Gauss–Newton's method and the CGLS inversion algorithm," *IEEE IEEE Trans. Antennas Propag.*, vol. 55, no. 8, pp. 2320–2331, Aug. 2007.

[2] C. Gilmore, P. Mojabi, A. Zakaria, S. Pistorius, J. LoVetri, "On super-resolution with an experimental microwave tomography system," *IEEE Antennas Wireless Lett.,* vol. 9, pp. 393 - 396, Apr. 2010.

[3] N. Simonov, S. I. Jeon , S. H. Son, J. M. Lee and H. J. Kim, "3D microwave breast imaging based on multistatic radar concept system," *Journal of the Korean Institute of Electromagnetic Engineering and Science*, vol. 12, no. 1, Mar. 2012, pp. 107-114.

[4] Qianqian Fang, *Computational methods for microwave medical imaging*, Ph. D. thesis, Dartmouth College, Hanover, Dec. 2004.

[5] P. C. Hansen, *Rank-Deficient and Discrete Ill-Posed Problems: Numerical Aspects of Linear Inversion*. SIAM, Philadelphia, 1997.

[6] J. G. Van Bladel, *Electromagnetic Fields,* 2nd ed., IEEE Press, 2007.